SUPPLEMENTARY MATERIALS

Transcriptional Patterns of Amygdala Functional Connectivity in First-episode, Drug-naïve Major Depressive Disorder

Liu et al.

Table of Contents

1. Supplementary Methods

I. Phenotypic and imaging dataset

Participants were selected from a publicly available brain imaging depression consortium (http://rfmri.org/REST-meta-MDD), comprising 1276 MDD patients and 1104 health controls (HC) [1,2]. Only unmedicated, first-episode MDD patients with the 17-item Hamilton Rating Scale for depression (HAMD) scores ≥ 14 were included. The exclusion criteria include the following aspects: (1) lack of information on sex, age, and education level; (2) age < 18 or > 65; (3) poor quality images [quality control (QC) scores < 4]; (4) excessive head motion [mean framewise displacement (FD) > 0.2 mm]. In addition, we did not include the sites with fewer than 10 MDD patients or 10 HC to balance the objectives of optimizing overall sample size with minimizing extreme biases [1]. The final analyzed sample included 210 MDD patients and age- and sex-matched 363 HC from four study sites. The screening process is summarized in a flow diagram in Figure S1. The demographic data and group differences by site can be found in Table S1. MDD diagnosis followed Diagnostic and Statistical Manual of Mental Disorders, Fourth Edition (DSM-IV) or International Classification of Diseases 10 (ICD-10) criteria. The depression severity was assessed by HAMD. HC had no history of psychiatric or neurological disorders. The study has been approved by the ethics committees of each site and written informed consent was received from each subject prior to the formal testing.

Brain image preprocessing utilized DPARSF software (http://www.rfmri.org/). The preprocessing steps were as follows: (1) remove the first 10 volumes. (2) slice timing

and motion correction. (3) covariate regression (white matter signal, cerebrospinal fluid (CSF) signal, and Friston-24 motion parameters) [3]. Global signal regression was omitted due to ongoing debate on its effects. (4) normalization to the Montreal Neurological Institute (MNI) template (3 mm × 3 mm × 3 mm) [4]. (5) temporal bandpass filtering (0.01-0.10 Hz). The key data acquisition parameters of each site can be found in Table S2.

II. Support vector machine

We employed amygdala functional connectivity to train support vector machine (SVM) classifiers using the MATLAB Classification Learner App (MATLAB 2022b), chosen for its widespread adoption in neuroimaging research [5]. SVM identifies a hyperplane maximizing the margin between binary classes in the feature space, enabling it to learn classification strategies from the training set, refine them with the validation set, and make individual classification decisions in the test set. The feature set comprised significantly different amygdala functional connectivity between the two groups, resulting in 11 features. Initially, the datasets were divided into training and test sets (7:3 ratio). Within the training set, we employed 10-fold cross-validation to further divide the data into internal training and validation sets (9:1 ratio) for model refinement. Finally, we assessed the model's performance using the test set, with the area under the receiver operating characteristic curve (AUC) and accuracy as key metrics for classification performance evaluation. AUC estimation was conducted by plotting a receiver operating characteristic (ROC) curve, depicting the classification performance across all thresholds based on the true positive rate and false positive

rate.

III. Transcription-neuroimaging association analysis

We conducted Pearson's correlation analysis to explore the relationship between the expression levels of 15,633 genes and the differences in amygdala functional connectivity between MDD and HC. Each column of the Z-score normalized gene expression matrix was considered as an independent variable, while the Z-score normalized amygdala functional connectivity case-control T-vector served as the dependent variable in the Pearson's correlation analysis. Genes with significant correlations (Benjamini-Hochberg false discovery rate corrected P-value < 0.05) were retained for further investigation.

Additionally, we employed a permutation test with 1,000 iterations to evaluate whether the number of identified genes exceeded what would be expected by chance [6]. Considering the spatial autocorrelation (SA) inherent in brain maps, we utilized the Brain Surrogate Maps with Autocorrelated Spatial Heterogeneity (BrainSMASH, https://github.com/murraylab/brainsmash) package to generate 1,000 surrogate maps preserving SA for the three actual amygdala functional connectivity difference maps [7,8]. Each permutation involved repeating the spatial correlation analyses and tallying the number of overlapping genes to establish a null distribution. By comparing the number of genes significantly associated with real amygdala functional connectivity difference maps to this null distribution, we assessed the statistical significance of our findings (permutation P-value < 0.05).

2. Supplementary Tables

Supplementary Table 1 Demographic and clinical characteristics of each site.

Site	Sex (M/F)	Age, year (Med (P25, P75))	Education level (year) (mean (SD))	HAMD (mean (SD))
1. MDD (n = 37)	13/24	30 (21, 43)	11.59 (3.57)	27.24 (6.40)
HC (n = 63)	26/37	28 (22, 39)	13.16 (2.46)	NA
2. MDD (n = 63)	21/42	30 (26, 35)	13.70 (3.37)	21.29 (3.45)
HC (n = 32)	15/17	28 (27, 32.75)	14.59 (2.82)	NA
3. MDD (n = 100)	32/68	37 (29, 48)	10.99 (3.68)	22.06 (4.14)
HC (n = 239)	79/160	42 (23, 56)	12.93 (3.94)	NA
4. MDD (n = 10)	6/4	22 (19.75, 25.25)	14.3 (1.70)	22.5 (6.10)
HC (n = 29)	11/18	27 (24, 47.5)	14.45 (4.16)	NA
All MDD (n = 210)	72/138	32 (26, 43)	12.07 (3.71)	22.76 (4.96)
All HC (n = 363)	131/232	31 (24, 50)	13.24 (3.69)	NA
P	0.664[a]	0.174[b]	< 0.001[c]	-

Abbreviations: HC, health controls; MDD, major depressive disorder; HAMD, the Hamilton Depression Rating Scale-17; M, male; F, female; Med, median; P25, 25th percentile; P75, 75th percentile; SD, standard deviation; NA, not available. Note: [a] Chi-square test; [b] Mann–Whitney U test; [c] Two-sample t-test.

Note: The four sites were respectively located in: 1) Department of Psychiatry, First Affiliated Hospital, China Medical University. 2) The Second Xiangya Hospital of Central South University; 3) Faculty of Psychology, Southwest University; 4) Mental Health Center, West China Hospital, Sichuan University.

Supplementary Table 2 The key data acquisition parameters of each site included in the study.

Site	MR Scanner	TR (ms)	TE (ms)	Slice number	Time points
1	GE Signa 3T	2000	30	35	200
2	Siemens Tim Trio 3T	2500	25	39	200
3	Siemens Tim Trio 3T	2000	30	32	242
4	Philips Achieva 3.0T TX	2000	30	38	240

Note: The four sites were respectively located in: 1) Department of Psychiatry, First Affiliated Hospital, China Medical University. 2) The Second Xiangya Hospital of Central South University; 3) Faculty of Psychology, Southwest University; 4) Mental Health Center, West China Hospital, Sichuan University.

Supplementary Table 3 Donor information for the Allen Human Brain Atlas.

Donor ID	Sex	Age (year)	Postmortem interval (h)	Handedness	Hemispheres	Samples
H0351.2001	M	24	23	Left	Both	946
H0351.2002	M	39	10	Left	Both	893
H0351.1009	M	57	25.5	Cross-dominant	Left	363
H0351.1012	M	31	17.5	Right	Left	529
H0351.1015	F	49	30	Right	Left	470
H0351.1016	M	55	18	Right	Left	501

Abbreviations: M, male; F, female.

3. Supplementary Figures

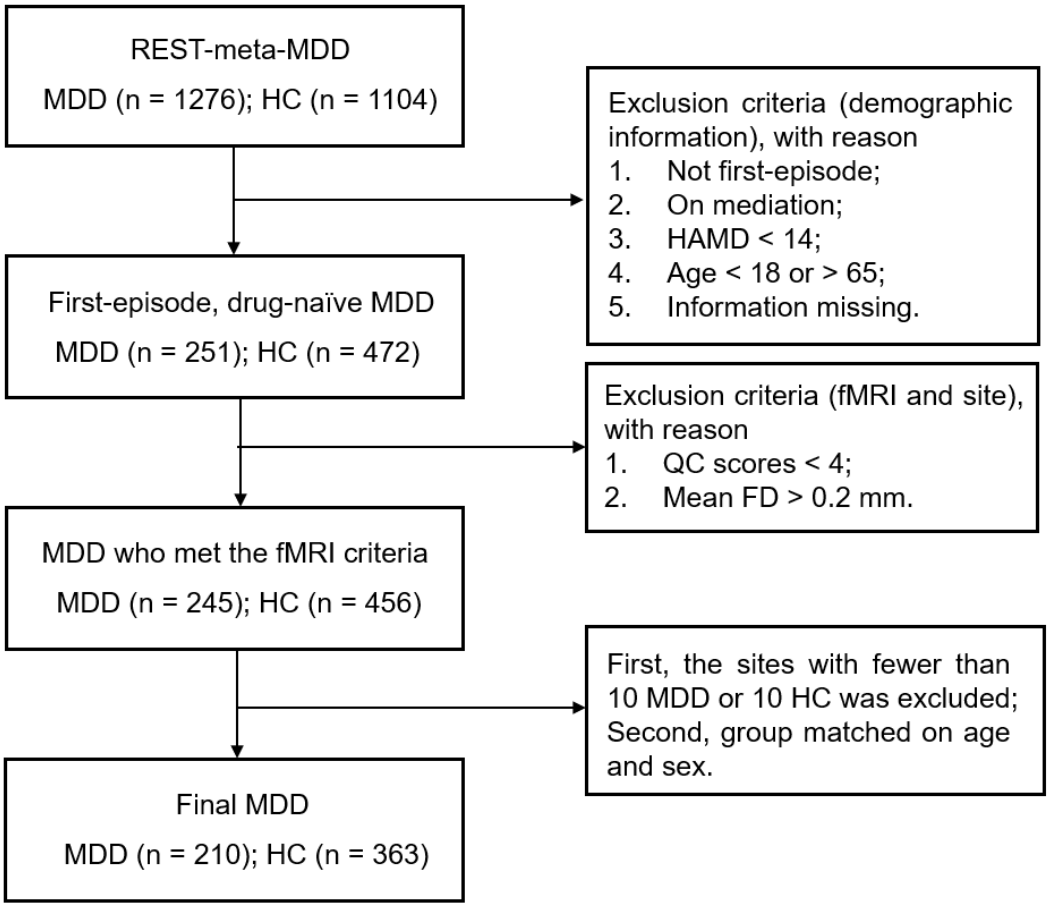

Supplementary Fig. 1 Flow chart of sample screening.

Abbreviations: HC, health controls; MDD, major depressive disorder; HAMD, the Hamilton Depression Rating Scale-17; QC, quality control; FD, framewise displacement.

Note: At each screening step, HC from sites without MDD patients were simultaneously excluded. Ultimately, our study included 210 patients with MDD and 363 HC across four sites.

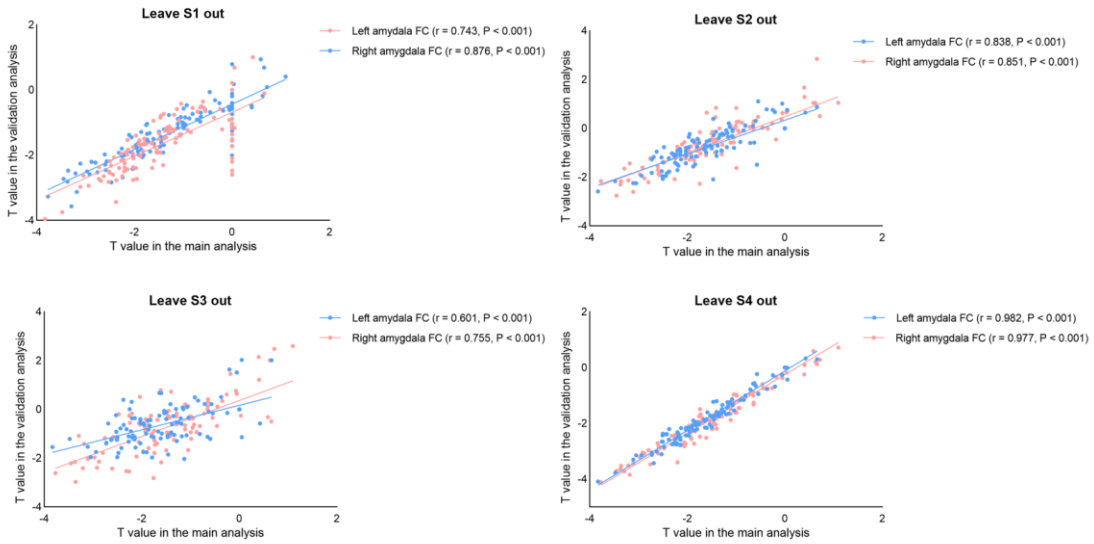

Supplementary Fig. 2 Spatial similarity of amygdala functional connectivity differences between validation analysis and main analysis. All the T-value maps from the validation analysis were significantly correlated with the corresponding T-value maps from the main analysis (all $P < 0.001$).

Abbreviations: Amygdala FC, amygdala functional connectivity.

Note: S1 was located in Department of Psychiatry, First Affiliated Hospital, China Medical University; S2 was located in Second Xiangya Hospital of Central South University; S3 was located in Faculty of Psychology, Southwest University; S4 was located in Mental Health Center, West China Hospital, Sichuan University.

4. Supplementary References

1 Yan CG, Chen X, Li L, Castellanos FX, Bai TJ, Bo QJ, et al. Reduced default mode network functional connectivity in patients with recurrent major depressive disorder. Proceedings of the National Academy of Sciences of the United States of America. 2019;116(18):9078-83.

2 Wang K, Hu Y, Yan C, Li M, Wu Y, Qiu J, et al. Brain structural abnormalities in adult major depressive disorder revealed by voxel- and source-based morphometry: evidence from the REST-meta-MDD Consortium. Psychological medicine. 2023;53(8):3672-82.

3 Ashburner J, Friston KJ. Unified segmentation. neuroimage. 2005;26(3):839-51.

4 Ashburner J. A fast diffeomorphic image registration algorithm. Neuroimage. 2007;38(1):95-113.

5 Orrù G, Pettersson-Yeo W, Marquand AF, Sartori G, Mechelli A. Using Support Vector Machine to identify imaging biomarkers of neurological and psychiatric disease: a critical review. Neuroscience and biobehavioral reviews. 2012;36(4):1140-52.

6 Cai M, Ji Y, Zhao Q, Xue H, Sun Z, Wang H, et al. Homotopic functional connectivity disruptions in schizophrenia and their associated gene expression. Neuroimage. 2024;289:120551.

7 Hawrylycz M, Miller JA, Menon V, Feng D, Dolbeare T, Guillozet-Bongaarts AL, et al. Canonical genetic signatures of the adult human brain. Nature neuroscience. 2015;18(12):1832-44.

8 Arnatkeviciute A, Fulcher BD, Fornito A. A practical guide to linking brain-wide gene expression and neuroimaging data. Neuroimage. 2019;189:353-67.